



## Full paper

## Resveratrol-loaded nanoemulsion prevents cognitive decline after abdominal surgery in aged rats

Fabricio M. Locatelli <sup>a</sup>, Takashi Kawano <sup>a,\*</sup>, Hideki Iwata <sup>a</sup>, Bun Aoyama <sup>a</sup>, Satoru Eguchi <sup>b</sup>, Atsushi Nishigaki <sup>a</sup>, Daiki Yamanaka <sup>a</sup>, Hiroki Tateiwa <sup>a</sup>, Marie Shigematsu-Locatelli <sup>a</sup>, Masataka Yokoyama <sup>a</sup>

<sup>a</sup> Department of Anesthesiology and Intensive Care Medicine, Kochi Medical School, Oko, Nankoku, Kochi 783-8505, Japan

<sup>b</sup> Department of Dental Anesthesiology, Tokushima University School of Dentistry, 3-18-15 Kuramoto, Tokushima, 770-8504, Japan

## ARTICLE INFO

## Article history:

Received 28 May 2018

Received in revised form

12 August 2018

Accepted 17 August 2018

Available online 25 August 2018

## Keywords:

Resveratrol

Neuroinflammation

Postoperative cognitive dysfunction

Microglia

## ABSTRACT

The maladaptive response of aged microglia to surgery and consequent neuroinflammation plays a key pathogenic role in postoperative cognitive dysfunction (POCD). Here, we assessed the preventive effect of resveratrol (RESV) for POCD in aged rats. The emulsified form of RESV (*e*-RESV) was selected to improve its oral and brain bioavailability. Animals were assigned to one of four groups: *e*-RESV (80 mg/kg) versus vehicle treatment by abdominal surgery versus isoflurane anesthesia alone ( $n = 8$  in each group). The dose-dependent effects of *e*-RESV were also assessed in dose range of 0–60 mg/kg. Either vehicle or *e*-RESV was administered intragastrically 24 h before surgery. Seven days after procedure, cognitive function was evaluated using a novel object recognition test, followed by measurement of hippocampal pro-inflammatory cytokine levels. Our results showed that pre-treatment with *e*-RESV attenuated the surgery-induced cognitive impairment and related hippocampal neuroinflammation at 40 mg/kg or higher doses. Additionally, the *ex-vivo* experiments revealed that the preemptive *e*-RESV regimen reduced the hippocampal microglial immune reactivity to lipopolysaccharide. Furthermore, *e*-RESV induced neuroprotective benefits were inhibited by the concomitant administration of sirtinol, a specific SIRT1 inhibitor. Our findings imply the preventive potential of *e*-RESV for POCD *via* the SIRT1 signaling pathway.

© 2018 The Authors. Production and hosting by Elsevier B.V. on behalf of Japanese Pharmacological Society. This is an open access article under the CC BY-NC-ND license (<http://creativecommons.org/licenses/by-nc-nd/4.0/>).

## 1. Introduction

There is an emerging concern that surgery may trigger and accelerate the age-related cognitive impairment, which is referred as postoperative cognitive dysfunction (POCD).<sup>1</sup> The development of POCD has been reported to be associated with long-term disability and increased mortality.<sup>2</sup> Although some preventive strategies for POCD have been proposed in preclinical studies, as well as small exploratory clinical trials, no established interventions are currently available.<sup>3,4</sup> Specifically, neuroinflammation, *i.e.*, a maladaptive microglial activation and overproduction of cytokines, is a key in the pathogenesis of neurodegenerative processes including Alzheimer's

disease (AD) and POCD.<sup>1,5–8</sup> Our recent study reported that the postoperative neuroinflammation may transit from acute to chronic in an age- and hippocampal-specific manner, resulting in the development of POCD.<sup>9</sup> Therefore, the acute neuroinflammation during the early postoperative period may be critical therapeutic target for POCD.

Resveratrol (RESV), a polyphenol present in red wine, is well-known to have beneficial biochemical properties, including anti-aging and anti-neuroinflammatory effects.<sup>10–12</sup> Indeed, a preclinical study reported the protective effects of 12 weeks oral RESV treatment on aging-induced cognitive impairment.<sup>12</sup> In addition, a clinical trial for AD showed that chronic oral treatment with RESV for 53 weeks reduces pro-neuroinflammatory factors in cerebrospinal fluid, improving cognitive function.<sup>13,14</sup> Differing from the long-term progression of normal aging and AD, POCD is a consequence of the acute neuroinflammatory response triggered by the surgical procedure.<sup>9</sup> Therefore, acute, high-dose regimen during perioperative period may be appropriate for POCD prevention. However, our preliminary

\* Corresponding author. Department of Anesthesiology and Intensive Care Medicine, Kochi Medical School, Kohasu, Oko-cho, Nankoku, Kochi, 783-8505, Japan. Fax: +81 88 880 2475.

E-mail address: [takashika@kochi-u.ac.jp](mailto:takashika@kochi-u.ac.jp) (T. Kawano).

Peer review under responsibility of Japanese Pharmacological Society.

study indicated that a preemptive injection with a single high-dose of free RESV, even at maximum administrable dose, failed to induce any neuro-cognitive protection in aged rats (Supplementary data 1). One plausible explanation for this may be due to the low bioavailability of RESV, particularly in the brain.<sup>15</sup> Alternatively, nanoemulsion based drug delivery systems has recently emerged as a promising strategy for overcome this issue, enhancing RESV solubility and improving permeation across the blood brain barrier.<sup>16–20</sup> Consistently, we hypothesized that nanoemulsified form of RESV can be effective for preventing the development of POCD.

RESV-induced neuroprotection is thought to be mainly mediated by allosteric activation of sirtuin-1 (silent mating type information regulation 2 homolog 1; SIRT1), a major gene associated with longevity.<sup>10,21</sup> SIRT1 is an evolutionarily conserved mammalian nicotinamide adenine dinucleotide-dependent protein deacetylase that is implicated in a wide range of aging-related diseases.<sup>22</sup> As SIRT1 is also reported to regulate microglial activity,<sup>23</sup> we further hypothesized that preoperative RESV treatment can act as an anti-neuroinflammatory agent *via* the SIRT1 pathway.

To test our hypothesis, we investigated the effects of a preoperative single dose of RESV-loaded nanoemulsion (emulsified RESV; *e*-RESV) on the development of POCD in an aged rat model of abdominal surgery. The effects of *e*-RESV on the microglial

phenotype in the hippocampus were also assessed in *ex-vivo* preparations.

## 2. Materials and methods

### 2.1. Animals and experimental designs

All experiments were approved by the Institutional Animal Care and Use Committee of Kochi Medical School. Wistar male rats aged 19–22 months were purchased from Alfresa Shinohara Chemicals Corporation (Kochi, Japan). The animals were divided into three sets of experiments (Fig. 1). Experiment-1 assessed the effects of *e*-RESV on POCD using a 2 × 2 experimental design: *e*-RESV (maximum dose; 80 mg/kg) versus vehicle emulsion of *e*-RESV (*e*-vehicle) treatment by abdominal surgery versus anesthesia alone (n = 8 in each group). Experiment-2 was conducted to observe the dose-dependent effects of *e*-RESV (0, 2.0, 20, 40, or 60 mg/kg; n = 6 in each dose group). In Experiment-3, to perform the SIRT1-related antagonist experiment using a specific SIRT1 inhibitor, sirtinol, surgical animals were randomly assigned to four treatment groups (n = 8 in each group): dimethyl sulfoxide (DMSO, a vehicle of sirtinol) with *e*-vehicle treated, sirtinol (5.0 mg/kg) with *e*-vehicle

#### A Experiment 1

##### *e*-RESV (mg/kg)

<i>e</i> -vehicle	24 h	Sham	7-day recovery
80	24 h	Sham	7-day recovery
<i>e</i> -vehicle	24 h	Surgery	7-day recovery
80	24 h	Surgery	7-day recovery

#### B Experiment 2

##### *e*-RESV (mg/kg)

<i>e</i> -vehicle	24 h	Surgery	7-day recovery
2.0	24 h	Surgery	7-day recovery
20	24 h	Surgery	7-day recovery
40	24 h	Surgery	7-day recovery
60	24 h	Surgery	7-day recovery

#### C Experiment 3

##### *e*-RESV (mg/kg)

DMSO	<i>e</i> -vehicle	24 h	Surgery	7-day recovery
Sirtinol	<i>e</i> -vehicle	24 h	Surgery	7-day recovery
DMSO	80	24 h	Surgery	7-day recovery
Sirtinol	80	24 h	Surgery	7-day recovery

Behavioral testing



Hippocampus extraction

Cytokine measurement

Microglial sensitivity

**Fig. 1. Schematic diagram of the three different experimental protocols.** (A) Experiment-1; Effects of emulsified resveratrol (*e*-RESV, 80 mg/kg) on postoperative cognitive impairment and related neuroinflammation (n = 8 in each group). (B) Experiment-2; Dose-dependent effects of *e*-RESV (0–60 mg/kg, n = 6 in each group). (C) Experiment-3; Antagonist study using sirtinol (n = 8 in each group).

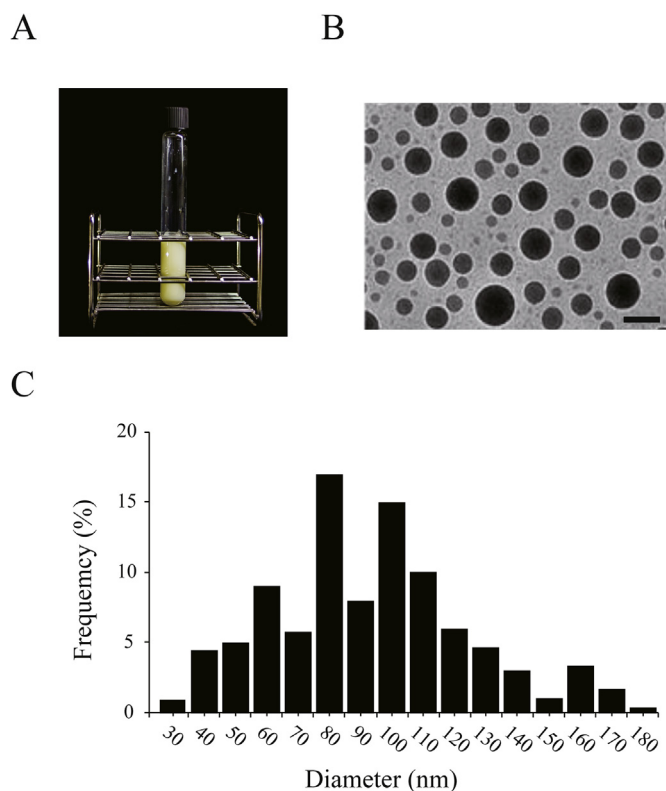


**Fig. 2. Emulsified resveratrol.** (A) Visual appearance. (B) Representative transmission electron microscope image. Nanoemulsion droplets appear as dark micelles. Scale bar: 100 nm. (C) Size-distribution histogram analyzed by ImageJ counting over 300 emulsified resveratrol nanoparticles from a series of TEM images.

treated, DMSO with *e*-RESV (80 mg/kg) treated, and sirtinol (5.0 mg/kg) with *e*-RESV (80 mg/kg) treated.

## 2.2. Experimental model of abdominal surgery

Abdominal surgery was performed as *per* our previous study.<sup>5</sup> Briefly, laparotomy consisted in a 2.0-cm midline longitudinal incision into the peritoneum, small intestine exteriorization and manipulation for 3 min. During the inhalation period of 15 min,

pulse rate, arterial oxygen saturation, and mean arterial blood pressure were measured noninvasively. Application of 0.2% ropivacaine (300  $\mu$ l) was used for postoperative analgesia as our previous study.<sup>24</sup> Postoperative pain was rated by the rat grimace scale (RGS).<sup>25</sup> Locomotor activity was evaluated using the open-field test on postoperative day 7 based on the total accumulated counts of horizontal beam crosses for 60 min.

## 2.3. Preparation and administration of *e*-RESV

*e*-RESV was prepared by the low-energy emulsification technique based on previous study.<sup>26</sup> Briefly, two oils, orange oil and grape seed oil, were mixed together for 1 h, and RESV (TCI Development Co., Ltd, China) was then added to produce a final concentration of 0.5 g/ml. Following overnight stirring, a nonionic surfactant, polyoxyethylene sorbitan monooleate (Tween<sup>®</sup> 80, Sigma–Aldrich, St. Louis, MO), was added to the solution. After another hour of mixing, the resulting organic phase was added drop-wise to the aqueous phase (5.0 mM phosphate buffer, pH = 7), while stirred at 500 rpm for 10-min. The emulsion without RESV was used as the control *e*-vehicle. Either *e*-vehicle or *e*-RESV was administered intragastrically by gavage 24 h before surgery. Sirtinol (Sigma–Aldrich) was dissolved in DMSO (Sigma–Aldrich) based on the previous study,<sup>27</sup> and administered by an *i.p.* injection 24 h before surgery. To confirm *e*-RESV establishment, the emulsion was imaged with transmission electron microscopy (TEM). Briefly, particles were mounted on a Cu grid with a Formvar and carbon supporting film and stained with a 2% uranyl acetate solution. After drying, the stained samples were observed under a JEM-1400Plus electron microscope (JEOL, Japan). The nanoparticle size distribution was determined by analyzing the acquired images with the ImageJ software (version 1.51, National Institutes of Health, Bethesda, MD, USA).

## 2.4. Novel object recognition task

One week after surgery, cognitive function was assessed using a novel object recognition test, similar with our previous study.<sup>5</sup> On the testing day, during the familiarization phase, the animal was allowed to freely explore the open-field arena containing two identical objects for 5 min. After 1 h, in the testing phase, the rat was placed into the experimental chamber again with a new set of objects containing one identical and one novel for 5 min. Object

**Table 1**  
Physiological parameters.

Group	Mean arterial pressure (mmHg)		Pulse rate (beats/min)		Oxygen saturation (%)		RGS	Total exploration time (seconds)
	Time 1	Time 2	Time 1	Time 2	Time 1	Time 2		
<b>Experiment-1</b>								
<i>e</i> -vehicle/sham	98.5 $\pm$ 9.7	95.4 $\pm$ 10.0	369.2 $\pm$ 21.4	377.5 $\pm$ 26.7	97.5 $\pm$ 1.7	97.6 $\pm$ 1.5	0.11 $\pm$ 0.07	51.7 $\pm$ 8.2
<i>e</i> -vehicle/surgery	99.7 $\pm$ 10.4	97.2 $\pm$ 9.1	385.4 $\pm$ 25.0	385.3 $\pm$ 25.4	98.0 $\pm$ 1.1	98.2 $\pm$ 1.6	0.17 $\pm$ 0.02	48.7 $\pm$ 7.0
<i>e</i> -RESV/sham	101.0 $\pm$ 12.5	99.0 $\pm$ 10.6	370.1 $\pm$ 24.5	363.8 $\pm$ 30.6	98.1 $\pm$ 1.2	98.1 $\pm$ 1.4	0.12 $\pm$ 0.03	52.0 $\pm$ 6.8
<i>e</i> -RESV/surgery	103.6 $\pm$ 10.3	100.7 $\pm$ 9.4	381.6 $\pm$ 29.3	370.9 $\pm$ 28.8	98.4 $\pm$ 1.0	98.5 $\pm$ 1.5	0.21 $\pm$ 0.06	50.6 $\pm$ 9.1
<b>Experiment-2</b>								
<i>e</i> -vehicle	96.4 $\pm$ 11.5	98.4 $\pm$ 7.7	375.2 $\pm$ 24.6	364.5 $\pm$ 25.4	97.2 $\pm$ 1.1	97.5 $\pm$ 0.9	0.14 $\pm$ 0.03	52.5 $\pm$ 10.4
<i>e</i> -RESV 2 mg/kg	95.2 $\pm$ 10.1	97.2 $\pm$ 8.0	387.5 $\pm$ 19.1	370.3 $\pm$ 29.6	97.6 $\pm$ 0.8	98.0 $\pm$ 0.9	0.19 $\pm$ 0.03	51.8 $\pm$ 8.0
<i>e</i> -RESV 20 mg/kg	101.7 $\pm$ 9.0	102.1 $\pm$ 8.8	370.3 $\pm$ 24.4	388.1 $\pm$ 27.1	98.1 $\pm$ 1.6	98.3 $\pm$ 1.7	0.15 $\pm$ 0.04	53.4 $\pm$ 7.1
<i>e</i> -RESV 40 mg/kg	95.3 $\pm$ 12.9	96.4 $\pm$ 10.6	381.0 $\pm$ 25.3	369.4 $\pm$ 30.2	98.0 $\pm$ 1.2	98.1 $\pm$ 1.1	0.14 $\pm$ 0.05	49.6 $\pm$ 6.6
<i>e</i> -RESV 60 mg/kg	94.6 $\pm$ 9.3	95.7 $\pm$ 8.7	370.6 $\pm$ 24.1	374.2 $\pm$ 25.0	98.4 $\pm$ 1.5	98.0 $\pm$ 1.4	0.20 $\pm$ 0.07	51.2 $\pm$ 7.8
<b>Experiment-3</b>								
DMSO/ <i>e</i> -vehicle	97.4 $\pm$ 8.5	99.5 $\pm$ 10.2	365.7 $\pm$ 19.6	367.4 $\pm$ 26.7	97.6 $\pm$ 1.5	97.8 $\pm$ 1.1	0.17 $\pm$ 0.05	56.7 $\pm$ 9.4
Sirtinol/ <i>e</i> -vehicle	100.7 $\pm$ 11.3	97.2 $\pm$ 8.7	374.9 $\pm$ 25.0	371.5 $\pm$ 31.5	97.3 $\pm$ 1.0	98.0 $\pm$ 1.2	0.15 $\pm$ 0.03	53.0 $\pm$ 6.8
DMSO/ <i>e</i> -RESV	93.1 $\pm$ 12.6	101.5 $\pm$ 7.9	371.0 $\pm$ 21.4	380.3 $\pm$ 25.1	97.9 $\pm$ 1.5	98.2 $\pm$ 1.0	0.18 $\pm$ 0.09	55.5 $\pm$ 7.0
Sirtinol/ <i>e</i> -RESV	95.5 $\pm$ 9.0	96.2 $\pm$ 8.4	381.6 $\pm$ 25.8	375.0 $\pm$ 27.6	98.2 $\pm$ 1.7	98.0 $\pm$ 0.8	0.14 $\pm$ 0.05	51.4 $\pm$ 7.9

Each parameter was recorded at Time 1 – after induction of anesthesia, before procedure, and at Time 2 – immediately after procedure, before termination of anesthesia. RGS: rat grimace scale assessed 2 h after surgery. Total exploration time: total time spent exploring the two objects during the familiarization phase of novel object recognition test. Data were expressed as the mean  $\pm$  standard deviation. Each group consisted of 8 animals.

exploration was defined as time spent sniffing the object with nose contact and/or within 1 cm. Recognition memory was expressed as the preference index; the ratio of time spent exploring an object during the familiarization phase or the novel object during the testing phase, over the total object exploration time.

### 2.5. Tissue collection and enzyme-linked immunosorbent assay

After behavior testing, animals were transcardially perfused, decapitated, and brains were harvested. The hippocampus was dissected, and then homogenized in ice-cold lysis buffer containing a protease inhibitor cocktail (P8340, Sigma–Aldrich). The hippocampal levels of interleukin-1 $\beta$  (IL-1 $\beta$ ) and tumor necrosis factor- $\alpha$  (TNF- $\alpha$ ) were analyzed using the ELISA kits for rat IL-1 $\beta$  (ER2IL1B, Thermo Scientific, USA) and TNF- $\alpha$  (438207, Biolegend, USA) according to the manufacturers' instructions. The data were normalized and expressed as pg TNF- $\alpha$  or IL-1 $\beta$  per mg tissue (pg/mg).

### 2.6. Isolation of hippocampal microglia

We further examined the effects of *e*-RESV on the pro-inflammatory phenotype of hippocampal microglia as previously described.<sup>5</sup> The hippocampus was digested with 0.1% trypsin and Dispase II (3.6 U/ml) for 1 h at 37 °C with shaking (100 strokes/min). The homogenates were centrifuged at 600  $\times$  g for 10 min at 4 °C. The pellets were re-suspended in 4 ml of 70% isotonic Percoll. The gradient was centrifuged at 2000  $\times$  g for 20 min. Microglial cells at the interface between the 70 and 37% Percoll layers were collected, and then plated at a density of 10<sup>4</sup> cells/100  $\mu$ l in DMEM containing 10% FBS. Before cell treatment, the medium was replaced with fresh serum-free medium followed by stimulation with lipopolysaccharide (LPS) at a concentration of 0.1, 1, 10, or 100 ng/ml, or media alone for 24 h at 37 °C in 5% CO<sub>2</sub>. The IL-1 $\beta$  and TNF- $\alpha$  levels in the culture medium were measured by ELISA.

### 2.7. Statistical analysis

All data were expressed as the mean  $\pm$  standard deviation (SD). For each dependent variable, group and/or other main effect(s) were tested with repeated measures ANOVA. Whenever ANOVA demonstrated significance, post hoc comparisons between the groups were performed in a pairwise manner by the Wilcoxon–Mann–Whitney test with Bonferroni correction. All data were analyzed using the statistical software SPSS (versions 11; SPSS Inc, Chicago, IL). Correlations between variables were analyzed by Pearson's correlation test.  $P < 0.05$  was considered significant.

## 3. Results

The TEM images revealed that the *e*-RESV particles has a spherical morphology (Fig. 2B). The histogram shows a size range from 23 nm to 181 nm, and 62% of the total population was <100 nm (Fig. 2C). The mean particle diameter was 86.4  $\pm$  12.7 nm (339 particles form 16 TEM images). All TEM images show almost an identical profile, indicating a high batch-to-batch reproducibility. In addition, no aggregations of *e*-RESV particles were visible under the optical microscope. These physicochemical features are largely consistent with a previous report.<sup>26</sup> No differences between groups in the physiological parameters during anesthesia and the RGS 2 h after surgery were observed (Table 1). In addition, the results of the open-field test conducted 6 days after surgery demonstrated no significant difference in any of the parameters measured within each treatment group (Supplementary data 2). Furthermore, the preemptive *e*-RESV regimen had no effect on blood coagulation parameters in aged rats (Supplementary data 3).

### 3.1. Novel object recognition performance

During the familiarization phase, there was neither intrinsic exploratory preference for either of the two objects nor significant difference in exploratory preference for the two objects in all groups. In addition, total exploration time did not differ within each treatment group (Table 1). These results implied that task motivation, curiosity, and ability during task performance were comparable among groups.

During the testing phase, the non-surgical control rats had a greater preference for the novel object compared with the familiar one (Fig. 3A, preference index: 77.3  $\pm$  6.8%). The rats in the surgical group exhibited significantly impaired novel object recognition performance (Fig. 3A, preference index: 55.1  $\pm$  8.2%,  $p < 0.05$  vs. non-surgical control rats). However, pre-treatment with *e*-RESV

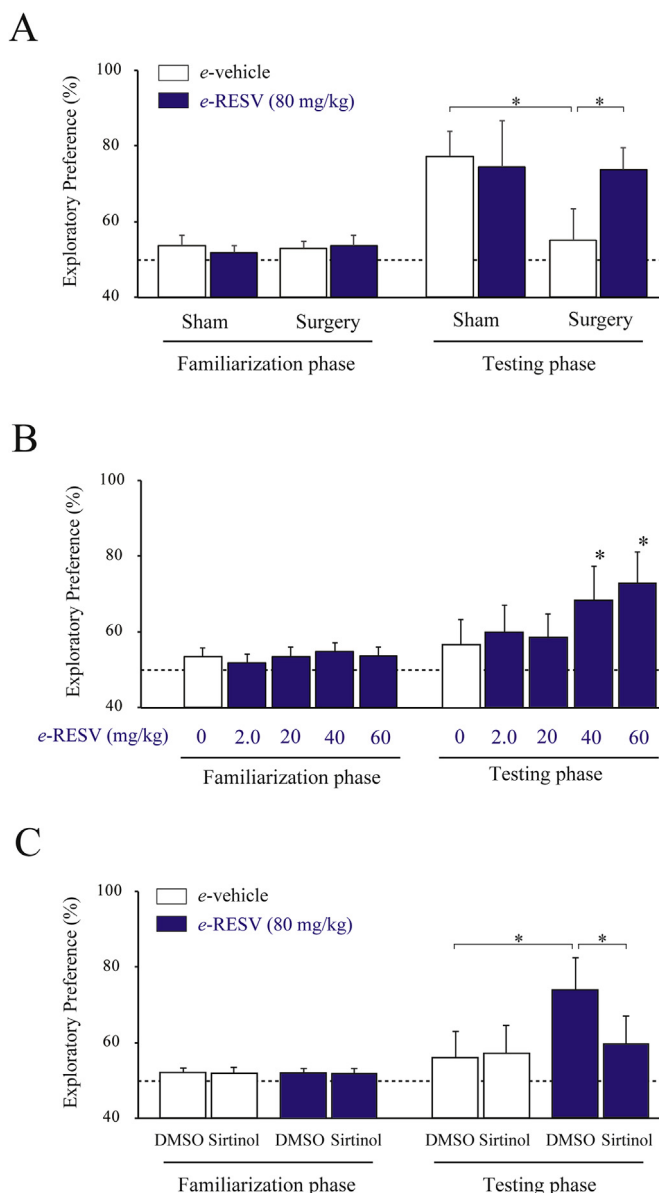


**Fig. 3. The results of the novel object recognition test.** The preference between two objects in the familiarization phase and testing phase of the novel object recognition test performed 7 days after sham or surgery is shown. Each vertical bar represents the mean  $\pm$  SD. (A) Experiment-1,  $n = 8$  in each group,  $*p < 0.05$ . (B) Experiment-2,  $n = 6$  in each group,  $*p < 0.05$  vs. *e*-RESV/0 mg/kg group. (C) Experiment-3,  $n = 8$  in each group,  $*p < 0.05$ .

significantly attenuated the surgery-induced cognitive impairment. In the dose-dependent experiment (Experiment-2), *e*-RESV inhibited surgery-induced memory deficit at 40 mg/kg or higher doses (Fig. 3B). Furthermore, in Experiment-3, although the sirtinol alone had no effect, it attenuated the effects of *e*-RESV (Fig. 3C). Neither *e*-RESV nor the surgical procedure had any significant influence on novel object recognition by adult rats (Supplementary data 4).

### 3.2. Levels of hippocampal cytokines

For the non-surgical rats, the average levels of hippocampal IL-1 $\beta$  and TNF- $\alpha$  were comparable between vehicle and *e*-RESV groups (Fig. 4A and Fig. 4B, respectively). However, for rats treated with the vehicle, levels of both cytokines were

significantly higher in the surgery group than in the non-surgery group. These increases in both IL-1 $\beta$  and TNF- $\alpha$  were inhibited in the surgery with *e*-RESV group. The anti-neuroinflammatory effects of *e*-RESV were dose-dependent (Experiment-2; Fig. 4C and D) and blocked by sirtinol (Experiment-3; Fig. 4E and F). Taking all experimental groups in Experiment-1 together, novel object recognition performance in the testing phase was inversely correlated with the hippocampal levels of both IL-1 $\beta$  (Fig. 5A,  $n = 32$ ;  $R^2 = -0.692$ ) and TNF- $\alpha$  (Fig. 5B,  $n = 32$ ;  $R^2 = -0.709$ ). In another experiment using sentinel animals, plasma cytokine levels increased after surgery, whereas these increases returned to baseline levels within 3 days after surgery (Supplementary data 5). In addition, *e*-RESV had no effect on plasma cytokine levels after surgery.

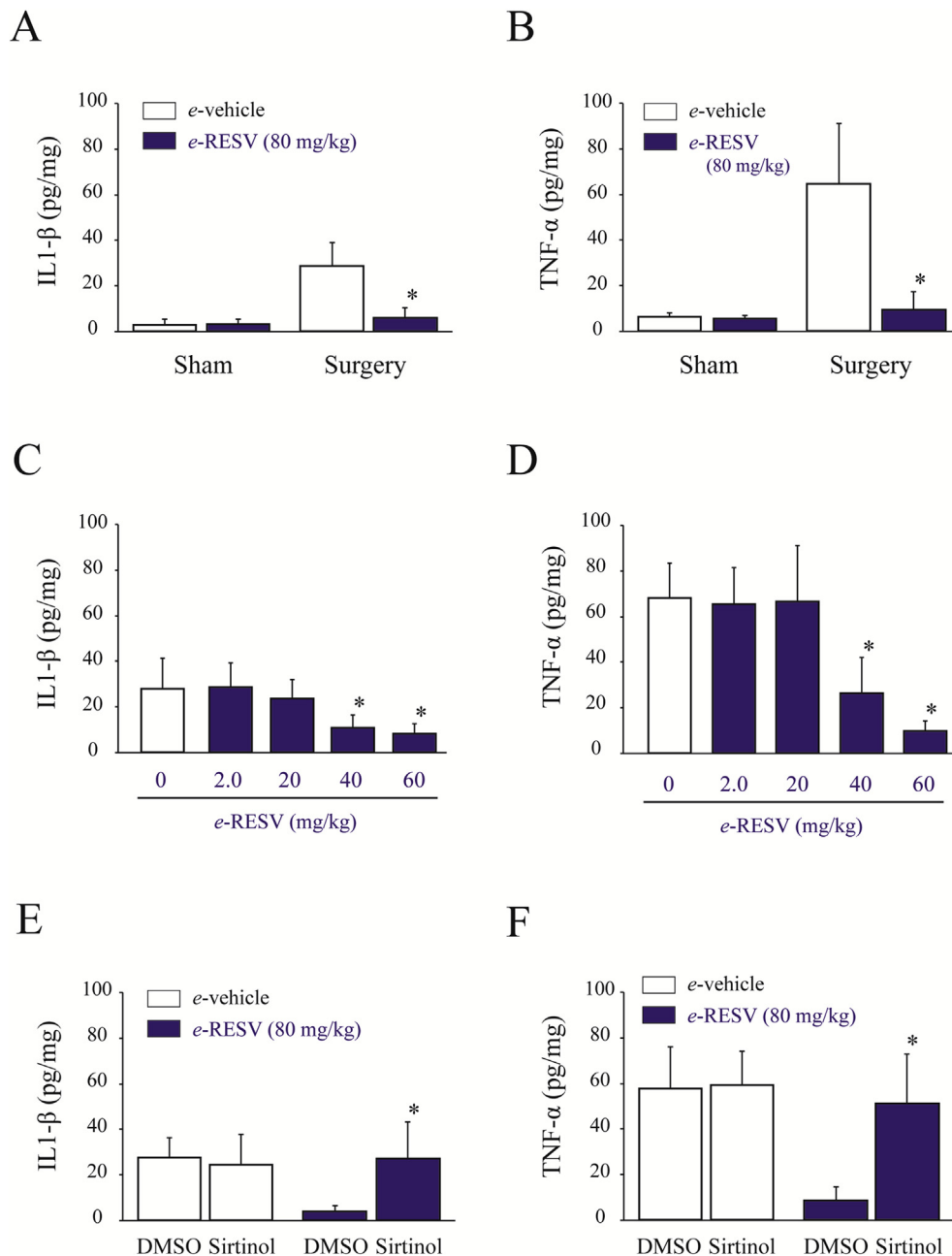


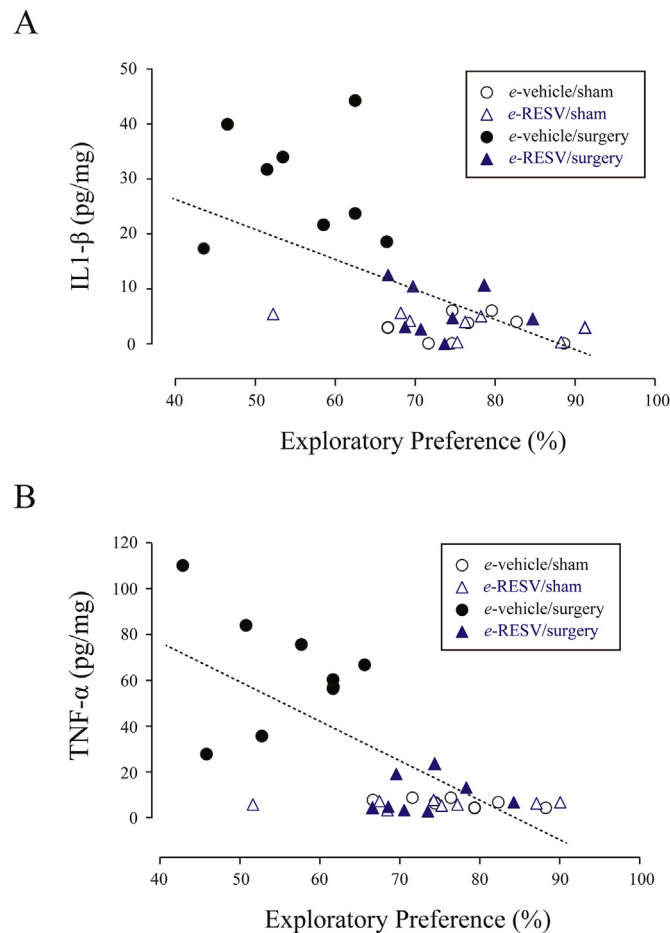
**Fig. 4.** The levels of proinflammatory cytokines in the hippocampus. The average levels of interleukin (IL)-1 $\beta$  and tumor necrosis factor (TNF)- $\alpha$  in each group in Experiment-1 (A and B,  $n = 8$  in each group,  $*p < 0.05$ ), Experiment-2 (C and D,  $n = 6$  in each group,  $*p < 0.05$  vs. *e*-RESV/0 mg/kg group), and Experiment-3 (E and F,  $n = 8$  in each group,  $*p < 0.05$ ) are shown. Each vertical bar represents the mean  $\pm$  SD.

### 3.3. Ex vivo microglial sensitivity to LPS

As the primary source for cytokines, microglia play as mediators of neuroinflammation.<sup>28</sup> Therefore, to investigate whether *e*-RESV influences microglial immunosensitivity, we measured the LPS sensitivity of hippocampal microglia isolated from animals in each group. In Experiment-1, there was no difference in baseline levels of IL-1 $\beta$  (Fig. 6A) and TNF- $\alpha$  (Fig. 6B) in all experimental groups. In microglia isolated from non-surgical groups, the LPS-induced increase in IL-1 $\beta$  was greatly attenuated in the *e*-RESV group compared with that in the vehicle group (Fig. 6A). On the other hand, the LPS-induced increase in IL-1 $\beta$  in the non-surgery with vehicle group was significantly exaggerated in the surgery with vehicle group. With respect to TNF- $\alpha$  levels, we found similar main effects among groups as those observed for IL-1 $\beta$ . Furthermore, the *e*-RESV-induced microglial anti-neuroinflammatory phenotype change was dose-dependent (Experiment-2; Fig. 6C and D), and attenuated by sirtinol (Experiment-3; Fig. 6E and F).

## 4. Discussion

In this study, we demonstrated that a prophylactic dose of *e*-RESV can prevent the development of cognitive deficits and related neuroinflammation in aged rats. The preoperative *e*-RESV regimen



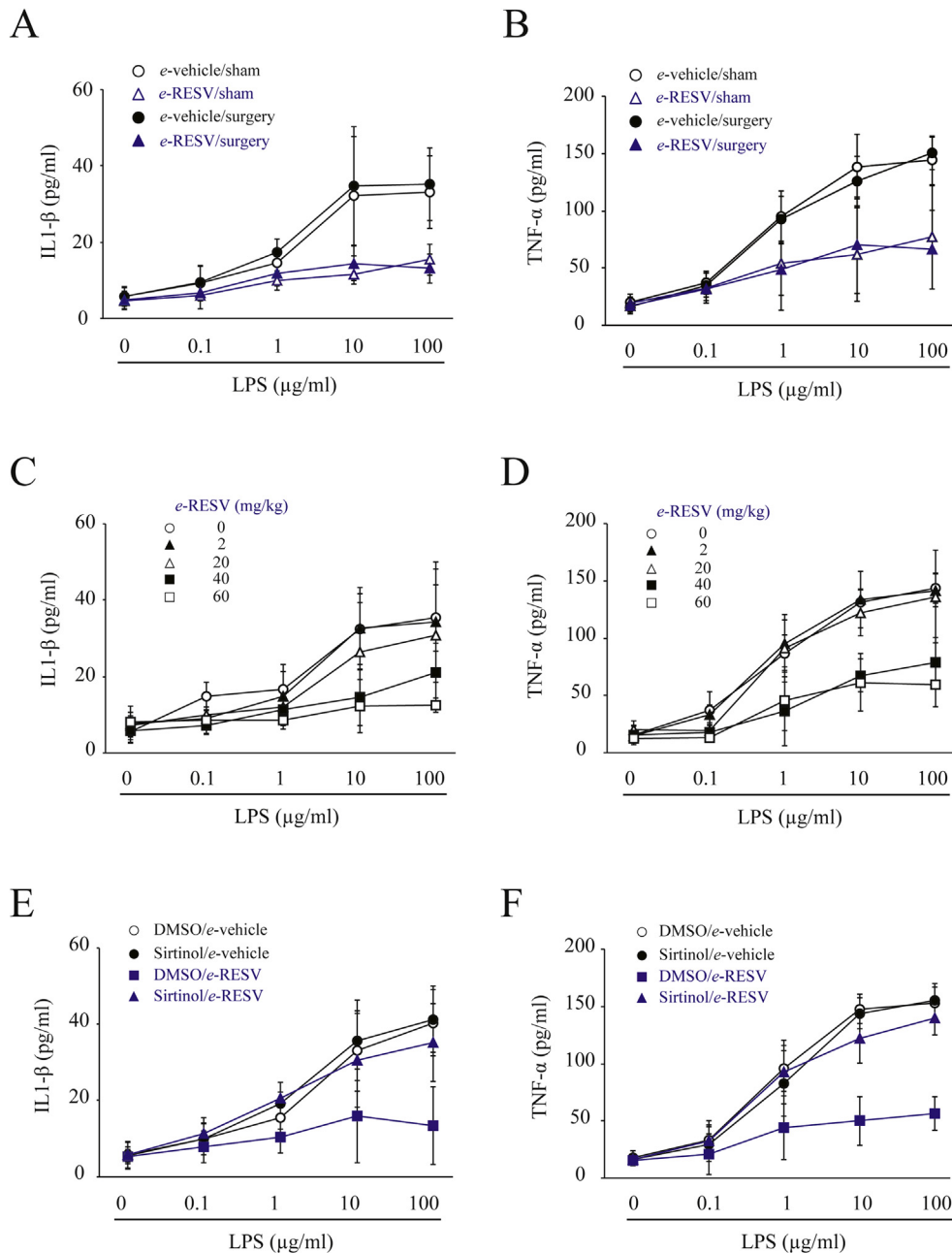


**Fig. 6.** Concentration–response effects of *ex vivo* stimulation with lipopolysaccharide (LPS) on the production of interleukin (IL)-1β and tumor necrosis factor (TNF)-α in cultured microglia. Hippocampal microglia were isolated from rats after the completion of cognitive testing in Experiment-1 (A and B, n = 8 in each group), Experiment-2 (C and D, n = 6 in each group), and Experiment-3 (E and F, n = 8 in each group). Cultured microglia were stimulated with 0.1, 1, 10, or 100 ng/ml, or media alone, and levels of IL-1β and TNF-α were measured from supernatants collected 24 h later. Each vertical bar represents the mean ± SD.

elimination from blood. Indeed, we found neither signs of bleeding nor changes in blood coagulation parameters in the *e*-RESV-treated surgical animals (Supplementary data 3). In addition, the *e*-RESV ingredients are widely used in cosmetics, food products, and pharmaceutical formulations. Nevertheless, the safety profile of *e*-RESV drug delivery system in human remains under investigated.

There are some limitations that should be addressed. First, we previously reported that neuroinflammation associated with POCD was found mainly in the hippocampus, and thus the present study focused on this brain region. However, *e*-RESV may interact with other brain regions. Second, since both TNF-α and IL-1β has been shown to play pivotal roles in neuroinflammation, we assessed

these two cytokines. However, other molecules are reported to be constitutively expressed in activated microglia. Third, previous studies reported that nanoemulsion drug delivery system could increase the brain bioavailability of RESV,<sup>18–20</sup> while actual *in vivo* pharmacokinetic data of *e*-RESV is currently lacking. In addition, our TEM analysis showed a positive dark staining of *e*-RESV particles despite the standard negative staining method (Fig. 2A). Indeed, mixed results, *i.e.*, dark and light staining, has been reported using similar technique, suggesting that the staining outcomes may depend on each chemical condition.<sup>34–36</sup> Furthermore, we cannot rule out the possibility for the oil phase to crystallize and form solid particles, increasing contrast in TEM. If that's

the case, the *in vivo* pharmacokinetics of *e*-RESV may be affected.<sup>37</sup> Therefore, future pharmacology and preclinical studies are needed before our findings can be translated into clinical practice.

In the present study, the hippocampal neuroinflammation-associated POCD was attenuated by a preemptive dose of *e*-RESV, but not by the free form of RESV. The *e*-RESV drug delivery system may enhance the brain bioavailability, and reduce the microglial immune sensitivity via the SIRT1 pathway. As the safety profile of RESV has been well-established, our approach warrants further study with respect to the translational potential for POCD clinical management.

### Conflicts of interest

All authors have no financial or scientific conflict of interest regarding the research described in this manuscript.

### Acknowledgements

This work was supported by a Grant-in Aid for Scientific Research (C): [Grant number 15K10538 to TK] from the Japan Society for the Promotion of Science, Tokyo, Japan. We are grateful to Dr. Dana Ulanova and Dr. Juan José Lauthier for their contributions and valuable comments. The TEM assistance of Dr. Shuji Sakamoto and Mr. Ken-ichi Yagyu is gratefully acknowledged.

### Appendix A. Supplementary data

Supplementary data related to this article can be found at <https://doi.org/10.1016/j.jphs.2018.08.006>.

### References

- Hovens IB, Schoemaker RG, van der Zee EA, Absalom AR, Heineman E, van Leeuwen BL. Postoperative cognitive dysfunction: involvement of neuroinflammation and neuronal functioning. *Brain Behav Immun*. 2014;38:202–210.
- Steinmetz J, Christensen KB, Lund T, Lohse N, Rasmussen LS. Long-term consequences of postoperative cognitive dysfunction. *Anesthesiology*. 2009;110(3):548–555.
- Papadopoulos G, Pouangare M, Papathanakos G, Arnaoutoglou E, Petrou A, Tzimas P. The effect of ondansetron on postoperative delirium and cognitive function in aged orthopedic patients. *Minerva Anestesiol*. 2014;80(4):444–451.
- Hovaguimian F, Tschopp C, Beck-Schimmer B, Puhon M. Intraoperative ketamine administration to prevent delirium or postoperative cognitive dysfunction: a systematic review and meta-analysis. *Acta Anaesthesiol Scand*. 2018;1–12.
- Kawano T, Eguchi S, Iwata H, Tamura T, Kumagai N, Yokoyama M. Impact of preoperative environmental enrichment on prevention of development of cognitive impairment following abdominal surgery in a rat model. *Anesthesiology*. 2015;123(1):160–170.
- Cibelli M, Fidalgo AR, Terrando N, et al. Role of interleukin-1beta in postoperative cognitive dysfunction. *Ann Neurol*. 2010;68(3):360–368.
- Terrando N, Monaco C, Ma D, Foxwell BM, Feldmann M, Maze M. Tumor necrosis factor- $\alpha$  triggers a cytokine cascade yielding postoperative cognitive decline. *Proc Natl Acad Sci U S A*. 2010;107(47):20518–20522.
- Locatelli FM, Kawano T. Postoperative cognitive dysfunction: preclinical highlights and perspectives on preventive strategies. In: Erbay RH, ed. *Current topics in anesthesiology*. Intech; 2017:129–144.
- Kawano T, Yamanaka D, Aoyama B, et al. Involvement of acute neuroinflammation in postoperative delirium-like cognitive deficits in rats. *J Anesth*. 2018;32:506–517.
- Lagouge M, Argmann C, Gerhart-Hines Z, et al. Resveratrol improves mitochondrial function and protects against metabolic disease by activating SIRT1 and PGC-1 $\alpha$ . *Cell*. 2006;127(6):1109–1122.
- Park SJ, Ahmad F, Philp A, et al. Resveratrol ameliorates aging-related metabolic phenotypes by inhibiting cAMP phosphodiesterases. *Cell*. 2012;148(3):421–433.
- Gocmez SS, Gacar N, Utkan T, Gacar G, Scarpace PJ, Tumer N. Protective effects of resveratrol on aging-induced cognitive impairment in rats. *Neurobiol Learn Mem*. 2016;131:131–136.
- Turner RS, Thomas RG, Craft S, et al. A randomized, double-blind, placebo-controlled trial of resveratrol for Alzheimer disease. *Neurology*. 2015;85(16):1383–1391.
- Moussa C, Hebron M, Huang X, et al. Resveratrol regulates neuro-inflammation and induces adaptive immunity in Alzheimer's disease. *J Neuroinflammation*. 2017;14(1):1.
- Shu XH, Wang LL, Li H, et al. Diffusion efficiency and bioavailability of resveratrol administered to rat brain by different routes: therapeutic implications. *Neurotherapeutics*. 2015;12(2):491–501.
- Arora D, Jaglan S. Therapeutic applications of resveratrol nanoformulations. *Environ Chem Lett*. 2018;16(1):35–41.
- Frezza RL, Bernardi A, Hoppe JB, et al. Neuroprotective effects of resveratrol against Abeta administration in rats are improved by lipid-core nanocapsules. *Mol Neurobiol*. 2013;47(3):1066–1080.
- Frezza RL, Bernardi A, Paese K, et al. Characterization of trans-resveratrol-loaded lipid-core nanocapsules and tissue distribution studies in rats. *J Biomed Nanotechnol*. 2010;6(6):694–703.
- Neves AR, Queiroz JF, Reis S. Brain-targeted delivery of resveratrol using solid lipid nanoparticles functionalized with apolipoprotein E. *J Nanobiotechnol*. 2016;14:27.
- Pangeni R, Sharma S, Mustafa G, Ali J, Baboota S. Vitamin E loaded resveratrol nanoemulsion for brain targeting for the treatment of Parkinson's disease by reducing oxidative stress. *Nanotechnology*. 2014;25(48):485102.
- Dai H, Sinclair DA, Ellis JL, Steegborn C. Sirtuin activators and inhibitors: promises, achievements, and challenges. *Pharmacol Ther*. 2018;188:140–154.
- Guarente L. Sirtuins in aging and disease. *Cold Spring Harb Symp Quant Biol*. 2007;72:483–488.
- Cho SH, Chen JA, Sayed F, et al. SIRT1 deficiency in microglia contributes to cognitive decline in aging and neurodegeneration via epigenetic regulation of IL-1 $\beta$ . *J Neurosci*. 2015;35(2):807–818.
- Chi H, Kawano T, Tamura T, et al. Postoperative pain impairs subsequent performance on a spatial memory task via effects on N-methyl-D-aspartate receptor in aged rats. *Life Sci*. 2013;93(25–26):986–993.
- Sotocinal SG, Sorge RE, Zaloum A, et al. The Rat Grimace Scale: a partially automated method for quantifying pain in the laboratory rat via facial expressions. *Mol Pain*. 2011;7:55.
- Davidov-Pardo G, McClements DJ. Nutraceutical delivery systems: resveratrol encapsulation in grape seed oil nanoemulsions formed by spontaneous emulsification. *Food Chem*. 2015;167:205–212.
- Shalwala M, Zhu SG, Das A, Salloum FN, Xi L, Kukreja RC. Sirtuin 1 (SIRT1) activation mediates sildenafil induced delayed cardioprotection against ischemia-reperfusion injury in mice. *PLoS One*. 2014;9(1), e86977.
- Wong WT. Microglial aging in the healthy CNS: phenotypes, drivers, and rejuvenation. *Front Cell Neurosci*. 2013;7:22.
- Saraiva C, Praca C, Ferreira R, Santos T, Ferreira L, Bernardino L. Nanoparticle-mediated brain drug delivery: overcoming blood-brain barrier to treat neurodegenerative diseases. *J Control Release*. 2016;235:34–47.
- Yen CC, Chang CW, Hsu MC, Wu YT. Self-nanoemulsifying drug delivery system for resveratrol: enhanced oral bioavailability and reduced physical fatigue in rats. *Int J Mol Sci*. 2017;18(9).
- Steinman L. Modulation of postoperative cognitive decline via blockade of inflammatory cytokines outside the brain. *Proc Natl Acad Sci U S A*. 2010;107(48):20595–20596.
- Lavan AH, Gallagher P. Predicting risk of adverse drug reactions in older adults. *Ther Adv Drug Saf*. 2016;7(1):11–22.
- Chiba T, Kimura Y, Suzuki S, Tatefuji T, Umegaki K. Trans-resveratrol enhances the anticoagulant activity of warfarin in a mouse model. *J Atheroscler Thromb*. 2016;23(9):1099–1110.
- Kumar R, Kaur K, Uppal S, Mehta S. Ultrasound processed nanoemulsion: a comparative approach between resveratrol and resveratrol cyclodextrin inclusion complex to study its binding interactions, antioxidant activity and UV light stability. *Ultrason Sonochem*. 2017;37:478–489.
- Zhang L, Tong H, Garewal M, Ren G. Optimized negative-staining electron microscopy for lipoprotein studies. *Biochim Biophys Acta Gen Subj*. 2013;1830(1):2150–2159.
- Silva HD, Cerqueira MA, Vicente AA. Influence of surfactant and processing conditions in the stability of oil-in-water nanoemulsions. *J Food Eng*. 2015;167:89–98.
- Bai L, McClements DJ. Extending emulsion functionality: post-homogenization modification of droplet properties. *Processes*. 2016;4(2):17.